Science Bulletin 64 (2019) 1902–1909

Contents lists available at ScienceDirect

Science Bulletin

journal homepage: www.elsevier.com/locate/scib

Article

Self-assembled sialyllactosyl probes with aggregation-enhanced properties for ratiometric detection and blocking of influenza viruses

Wei-Tao Dou [a], Zhao-Yang Qin [a], Jun Li [b], Dong-Ming Zhou [b], Xiao-Peng He [a,*]

[a] Key Laboratory for Advanced Materials, Feringa Nobel Prize Scientist Joint Research Center, School of Chemistry and Molecular Engineering, East China University of Science and Technology, Shanghai 200237, China
[b] Vaccine Research Center, Key Laboratory of Molecular Virology & Immunology, Institut Pasteur of Shanghai, Chinese Academy of Sciences, Shanghai 200031, China

ARTICLE INFO

Article history:
Received 20 June 2019
Received in revised form 30 July 2019
Accepted 14 August 2019
Available online 19 August 2019

Keywords:
Vibration-induced emission
Influenza viruses
Ratiometric
Fluorescence
Glycoprobe

ABSTRACT

Infection and dissemination of influenza viruses (IVs) causes serious health concerns worldwide. However, effective tools for the accurate detection and blocking of IVs remain elusive. Here, we develop a new sialyllactosyl probe with self-assembled core-shell structure for the ratiometric detection and blocking of IVs. *N*,*N*′-diaryl-dihydrodibenzo[*a*,*c*]phenazines were used to form the core structure by hydrophobic assembly in an aqueous solution with an aggregation-enhanced blue fluorescence mission. Subsequently, dicyanomethylene-4*H*-pyran-based sialyllactosides were used for self-assembly with the core structure, producing the sialyllactosyl probe that emits a red fluorescence due to Förster resonance energy transfer. The probe developed has been proven to be available for (1) the fluorescence ratiometric detection of IVs through selective interaction with the sialyllactosyl-binding proteins on the virus surface, and (2) effectively blocking the invasion of human-infecting IVs towards host cells as accentuated by the sialyllactosides on the surface of the probes.

1. Introduction

Influenza pandemics occurs seasonally worldwide, leading to a high mortality rate and significant economic loss [1–4]. Influenza A viruses (IVs) can be divided into two different subtypes in terms of the sialylglycan-binding affinity of their surface-bound hemagglutinin (HA). The avian IVs that predominantly recognize α2,3-sialylglycans transmit among birds and the human IVs that bind α2,6-sialylglycans have the capacity to infect humans [5–7]. It is reported that a certain number of avian IVs, upon mutations and re-assortments, show a switched sialylglycan-binding specificity, thus increasing the risk of human infection [8,9]. As a result, the effective identification of the different HA specificities of IVs can contribute to the timely warning of influenza pandemics. Unfortunately, the currently used analytical methods for IV detection including polymerase chain reaction, enzyme-linked immunosorbent assay, and virus isolation assay are complicated and time-consuming, which are not practically suitable for low-income regions. Additionally, the drug-resistance of some IV strains against first-line antiviral drugs also makes the development of new IV blocking agents urgently needed.

Supramolecular self-assembly is a simple yet effective method to construct functional materials using ordered molecular aggregation. When properly devised, functionally diverse compounds can be hierarchically weaved through non-covalent forces [10], leading to enhanced properties for a wide variety of applications. Recently, a number of elegant supramolecular materials have been designed and constructed for biomedical uses [11–13]. These include fluorescent multilayer microcapsules and organic Janus microspheres formed by hydrogen bonding and electrostatic interactions [14–17], fluorescent J-aggregates formed by π-π stacking [18], chirality-driven self-sorting supramolecular materials [19], metallacycle-cored supramolecular assemblies [20], and other forms of nanoparticles [21,22] and nanospheres [23] based on host-guest supramolecular interactions. However, supramolecular materials suitable for IV detection and blocking remain exclusive. Recently, we have developed self-assembled fluorescent probes for IVs based on thin-layer molybdenum disulfide [24] or conjugated polymers [25] as the backbone, on which sialyllactosyl probes were non-covalently conjugated. Comparing to synthetic small molecules, the structural homogeneity of inorganic and macromolecular materials is relatively more difficult to be exquisitely controlled. This might cause problems in quality control of products for clinical use.

To address this issue, here we developed a core-shell sialyllactosyl probe self-assembled from two individual small-molecule

SPECIAL ISSUE: Emerging Investigators 2019

* Corresponding author.
E-mail address: xphe@ecust.edu.cn (X.-P. He).

https://doi.org/10.1016/j.scib.2019.08.020
2095-9273/

probes for the ratiometric detection and blocking of IVs. Recently, Tian and co-workers [26] synthesized *N*,*N*′-diaryl-dihydro dibenzo [*a*,*c*]phenazines (**VR**) (Fig. 1a) as a new class of functional materials with unique optical properties. They demonstrated that these vibrionic compounds exhibited a fluorescence emission shift from red to blue upon molecular aggregation [27], thus making possible the development of fluorescence ratiometric probes based on the modulation of single-molecular vibration [28]. In the present study, **VR** was used to form the core structure of the probe in an aqueous solution by hydrophobic aggregation, leading to a drastically enhanced blue fluorescence emission because of a restriction of molecular vibration (Fig. 1b). Subsequently, dicyanomethylene-4*H*-pyran (DCM)-based sialyllactosides (Fig. 1a) were used for self-assembly with the **VR** core, producing the sialyllactosyl probe that emits a red fluorescence because of Förster resonance energy transfer (FRET) from **VR** to DCM (Fig. 1b). The self-assembled probe was shown to produce a ratiometric fluorescence detection signal for IVs through binding to the HA on the virus surface (Fig. 1b). Furthermore, the probe that displays sialyllactosides in a multivalent manner also showed strong capacity for blocking the entry of IVs into human host cells through antagonizing the interaction between HA and cell-surface sialylglycans (Fig. 1c).

2. Experimental

2.1. Fluorescence titration of VR with DCM23/DCM26

VR was dissolved in a phosphate buffered saline (PBS, 0.01 mol/L, pH 7.4, 1% DMSO, v:v) as solution at an initial concentration of 10 μmol/L, to which an increasing concentration of **DCM23** or

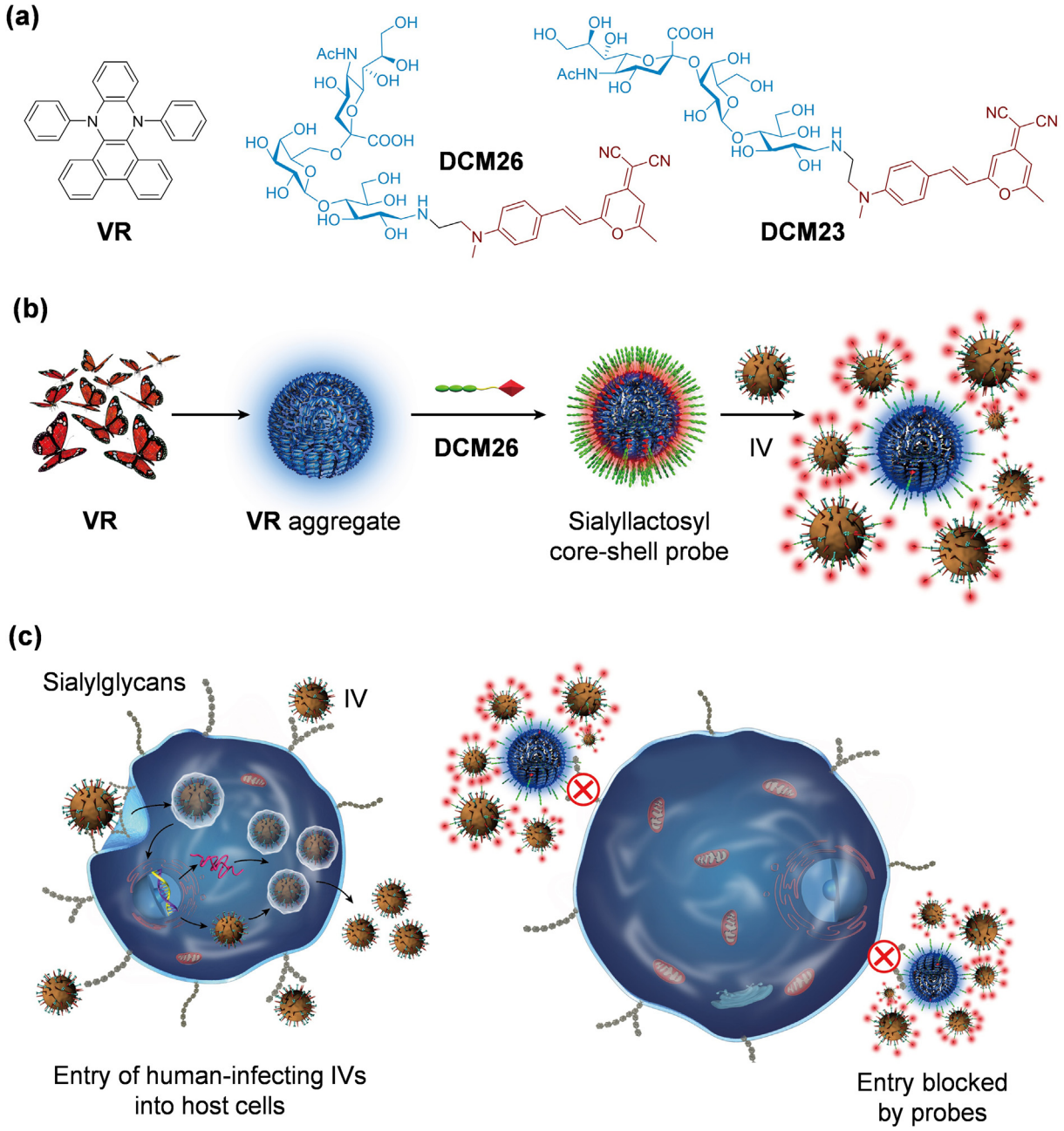

Fig. 1. (Color online) (a) Chemical structures of **VR**, **DCM26** and **DCM23**. (b) Schematic representation of the step-wise self-assembly between **VR** and **DCM26**, producing the core-shell sialyllactosyl probe for the fluorescence ratiometric detection of influenza viruses (IVs). (c) Use of the probe for the blocking of the entry of human-infecting IVs into host cells.

DCM26 was added (0–10 μmol/L). The mixture was incubated at room temperature for 30 s, and then the fluorescence was measured on a Varian Cary Eclipse fluorescence spectrophotometer with an excitation of 365 nm.

2.2. Fluorescence ratiometric detection of influenza viruses (IVs)

To a PBS solution (0.01 mol/L, pH 7.4, 1% DMSO, v:v) of **DCM23** or **DCM26** probe, IVs (H3N2, H7N9, H10N8, H1N1pdm09 or H5N1) of different concentrations were added. The resulting mixture was shaken for 5 min, and then the fluorescence was measured on a Varian Cary Eclipse fluorescence spectrophotometer with an excitation of 365 nm.

For other experimental details, see the Supporting Information associated with this article (online).

3. Results and discussion

VR [26] and the DCM-based sialyllactosides (**DCM26** and **DCM23** modified with α-2,6-sialyllactose and α-2,3-sialyllactose, respectively) [29] (Fig. 1a), were synthesized according to our previous report. **VR** was first dissolved in DMSO, and then dispersed in phosphate buffered saline (PBS, 0.01 mol/L, pH 7.4, 1% DMSO, v:v) to form aggregates with a restricted molecular vibration, leading to a strong blue fluorescence emission [28]. Subsequently, **DCM23** or **DCM26** was added to the aqueous solution of **VR**, producing the self-assembled sialyllactosyl probes (**VR**/**DCM23** and **VR**/**DCM26**) through an interaction between the DCM dye and the hydrophobic cavities of **VR** aggregates (Fig. 1b).

To characterize the self-assembly, a series of techniques were used. First, the UV–vis absorption and fluorescence spectra of **VR** and **DCM26** were measured (Fig. S1 online). We observed that the emission of **VR** well-overlapped the absorption of DCM, suggesting that the two fluorophores are potential FRET pairs. Then, a fluorescence titration assay was carried out by addition of increasing **DCM26** or **DCM23** to **VR** in order to prove the production of FRET between the two closely attached fluorophores after self-assembly. Excited by the absorption maxima of **VR** (365 nm), we observed that the initial fluorescence emission intensity of **VR** at 470 nm significantly decreased with that of **DCM26** and **DCM23** (at 600 nm) simultaneously increased in a concentration-dependent manner (Fig. 2a and b). This is characteristic of a FRET process from the blue-emitting **VR** to the red-emitting DCM. The quantum yield of **VR**/**DCM23** and **VR**/**DCM26** was determined to be 5.4% and 5.7%, respectively.

To further understand the mechanism of the fluorescence emission shift, the fluorescence lifetime of DCM and the self-assembled probe was measured. In a typical FRET process, the lifetime of the FRET donor is decreased with that of the FRET acceptor increased [30]. Using the excitation wavelength of **VR** (365 nm), we observed a lifetime decay of the self-assembled probes ($\tau_{\mathbf{VR/DCM23}}$ and $\tau_{\mathbf{VR/DCM26}}$ are 18.88 and 18.51 ns with excitation wavelength of 365 nm, respectively, Fig. S2 online). Meanwhile, by excitation

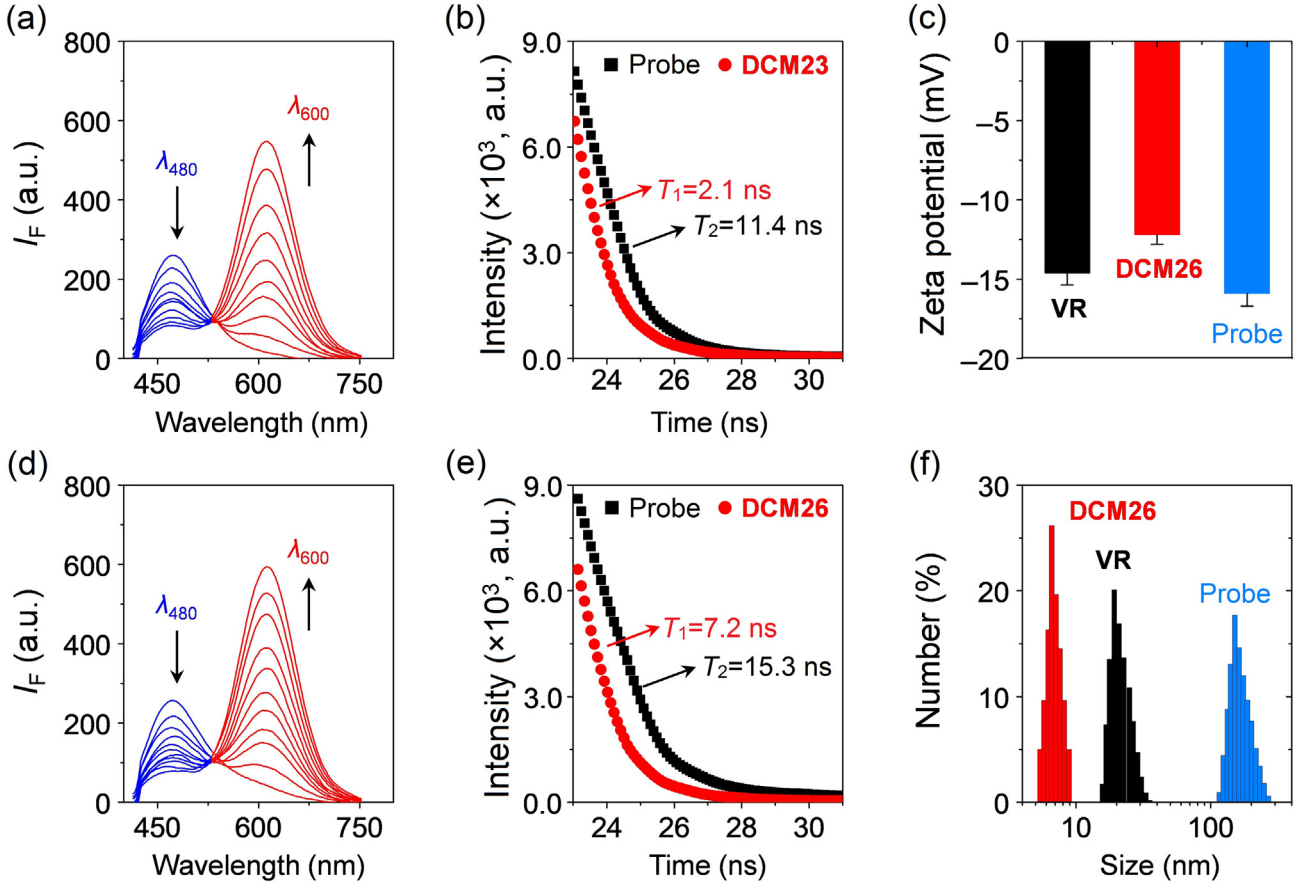

Fig. 2. (Color online) Fluorescence change of **VR** (10 μmol/L) in the presence of (a) increasing **DCM23** (0–10 μmol/L) and (d) increasing **DCM26** (0–10 μmol/L) in PBS (0.01 mol/L, pH 7.4, 1% DMSO, v:v); excitation wavelength = 365 nm. Fluorescence lifetime measurement of (b) **DCM23** (10 μmol/L) and **VR**/**DCM23** probe (10 μmol/L/10 μmol/L) and (e) **DCM26** (10 μmol/L) and **VR**/**DCM26** probe (10 μmol/L/10 μmol/L) in PBS (0.01 mol/L, pH 7.4, 1% DMSO, v:v); excitation wavelength = 460 nm. (c) Zeta potential of **VR** (10 μmol/L), **DCM26** (10 μmol/L) and **VR**/**DCM26** probe (10 μmol/L/10 μmol/L) measured in PBS (0.01 mol/L, pH 7.4, 1% DMSO, v:v). (f) Hydrodynamic parameter of **VR** (10 μmol/L), **DCM26** (10 μmol/L) and **VR**/**DCM26** probe (10 μmol/L/10 μmol/L) measured in PBS buffer (0.01 mol/L, pH 7.4, 1% DMSO, v:v).

with the absorption maxima (460 nm) of DCM (FRET doner), the fluorescence lifetime of **VR**/**DCM23** (11.4 ns, Fig. 2b) and **VR**/**DCM26** (15.3 ns, Fig. 2e) was determined to be longer than that of **DCM23** (2.1 ns) and **DCM26** (7.2 ns) alone, respectively. This is in accordance with previous experimental observations that the lifetime of the FRET donor (**VR**) and acceptor (DCM) is decreased and increased during a FRET process, respectively [14].

Subsequently, the zeta potential of **VR** before and after assembly with **DCM26** was measured (Fig. 2c). We observed that the electronegativity of **VR** was increased after assembly with **DCM26**; the increased absolute value of zeta potential of the probe with respect to **VR** aggregates alone suggests an increased stability of the self-assembled system [31]. The hydrodynamic diameter of **DCM26** in PBS was determined to be as low as ca. 5 nm due to its good dispersibility in the presence of the highly hydrophilic sialyllactosyl group (Fig. 2f). The particle diameter of **VR** aggregate in the aqueous medium was found to be ca. 20 nm as a result of its hydrophobic structure. In contrast, the diameter of the self-assembled **VR**/**DCM26** probe increased significantly to ca. 200 nm, suggesting that the self-assembly largely changed the molecular alignment of the assemblies of the two compounds. The binding constants between **VR** and DCM were also determined using the Lineweaver-Burk plot. A binding constant (K) of 3.12×10^4 and 4.17×10^4 L/mol was determined for the **VR**/**DCM23** (Fig. S3a online) and **VR**/**DCM26** (Fig. S3b online) probes, respectively. In addition, the self-assembled probes also showed good stability in PBS over a wide range of increasing pH (Fig. S4a online) and ionic strength (Fig. S4b online), two factors that can significantly compromise the structural integrity of self-assembled materials.

The morphology of the self-assembled **VR**/**DCM26** was characterized by different microscopic techniques including transmission electron microscopy (TEM), high-resolution scanning electron microscopy (HRSEM) and confocal laser-scanning microscopy (CLSM) (Fig. 3). We observed that free **VR** molecules spontaneously assembled into hexagonal aggregates (TEM) with strong blue emission (CLSM) in PBS. Note that the particle size of **VR** aggregates was observed to be much larger than that determined by DLS, which could be ascribed to the crystallization of the hydrophobic compounds on the solid phase required for the microscopic analyses.

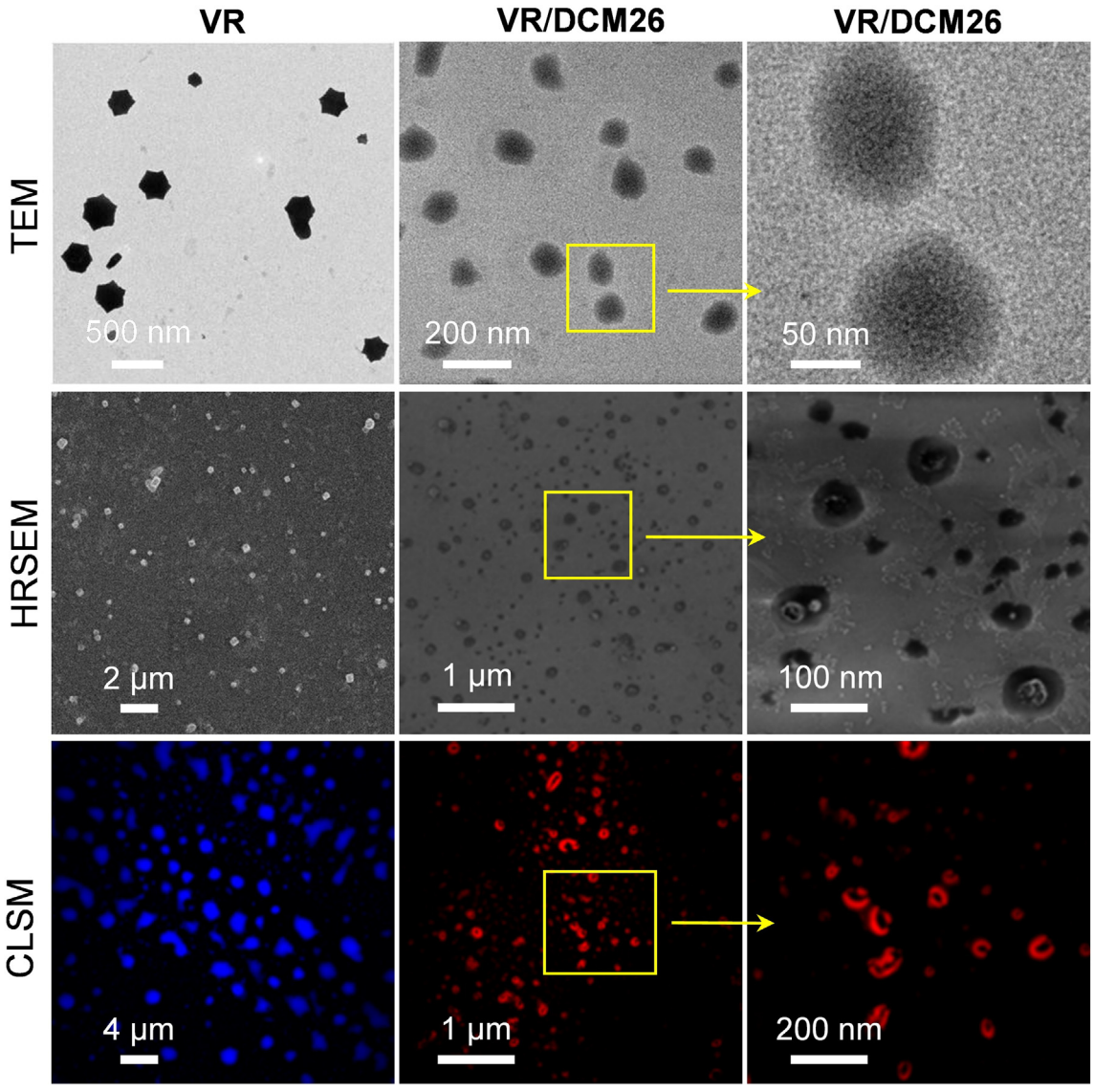

Fig. 3. (Color online) Morphological characterization of **VR** aggregates (10 μmol/L) and the core-shell probes (**VR**/**DCM26** = 10 μmol/L/10 μmol/L) using transmission electron microscopy (TEM), high-resolution scanning electron microscopy (HRSEM) and confocal laser-scanning microscopy (CLSM). For CLSM, the excitation channel used is 425–475 nm, and the emission channel used is 500–550 and 570–620 nm for **VR** and DCM, respectively.

After addition of **DCM26**, particles of a smaller size were formed (TEM). Interestingly, in their representative HRSEM images, we observed typical core-shell like particles with the fluorescence emission of the shell being that of DCM (CLSM). These data corroborate the self-assembly between **VR** aggregates and DCM sialyllactosides, producing sialyllactosyl probes with a core-shell particle-like architecture. This also corroborates the structural re-alignment of the assemblies between the two compounds as suggested by DLS.

With the self-assembled probes in hand, we tested their capacity for the detection of IVs. It is known that the membrane-bound HA determines the nature of host infection of IVs [32]. For example, the human IV H3N2 selectively binds to α-2,6-linked sialyl-glycans expressed in the upper respiratory of humans and the avian IV H10N8 interacts with α-2,3-linked sialyl-glycans existed in birds [33–35]. Consequently, we used IV stains of different HA binding specificities to determine the sensitivity of the probes. Three known IV strains, H3N2 (A/Beijing/353/89, human influenza), H10N8 (Lake/Hunan/3-9/2007, avian influenza) and H7N9 (A/Anhui/1/2013, human/avian influenza) were deactivated prior to use. We observed that after addition of H3N2 and H10N8 to the PBS solution of **VR**/**DCM26** (Fig. 4b) and **VR**/**DCM23** (Fig. 4d), respectively, the fluorescence emission intensity of DCM (600 nm) decreased while that of **VR** increased (480 nm). In contrast, only a slight fluorescence variation (decrease) was observed for both probes when the IVs were added reversibly (i.e., addition of H10N8 and H3N2 to **VR**/**DCM26** (Fig. 4a) and **VR**/**DCM23** (Fig. 4e), respectively). This preliminarily suggests the selective association between the sialyllactosyl groups on the shell surface of the probes with HA of the IVs, leading to detachment of the DCM sialyllactosides from the **VR** core. This subsequently interrupted the FRET mechanism between DCM and **VR**, causing the fluorescence of the latter to recover. Indeed, this hypothesis was further corroborated by the observation that presence of the human/avian dual-specific H7N9 IV strain led to the fluorescence ratiometric change of both **VR**/**DCM26** (Fig. 4c) and **VR**/**DCM23** (Fig. 4f) probes.

To better corroborate the interaction manner between probe and IV, TEM and CLSM were used. We observed that the treatment of **VR**/**DCM26** with specific IVs including H3N2 and H7N9 led to an obvious agglomeration of the virus particles as determined by both TEM and DLS (Fig. S5a online). In contrast, the incubation of the probe with the non-specific H10N8 only cause a slight change in diameter of the IV particles (Fig. S5b online), which might be cause by non-specific collisions between the viruses and probe particles. However, this did not cause the blue fluorescence of the probe to enhance (Fig. 4a), suggesting the stability of the core-shell structure formed. In their representative CLSM images (with VR excitation), we also observed a strong **VR** emission when treating **VR**/**DCM26** with H3N2 and H7N9 with the DCM emission being almost absent (Fig. 5). On the contrary, a typical DCM emission was observed for the probe after being treated with the non-specific H10N8 with the **VR** emission being undetectable. These results proved that the fluorescence ratiometric change of the

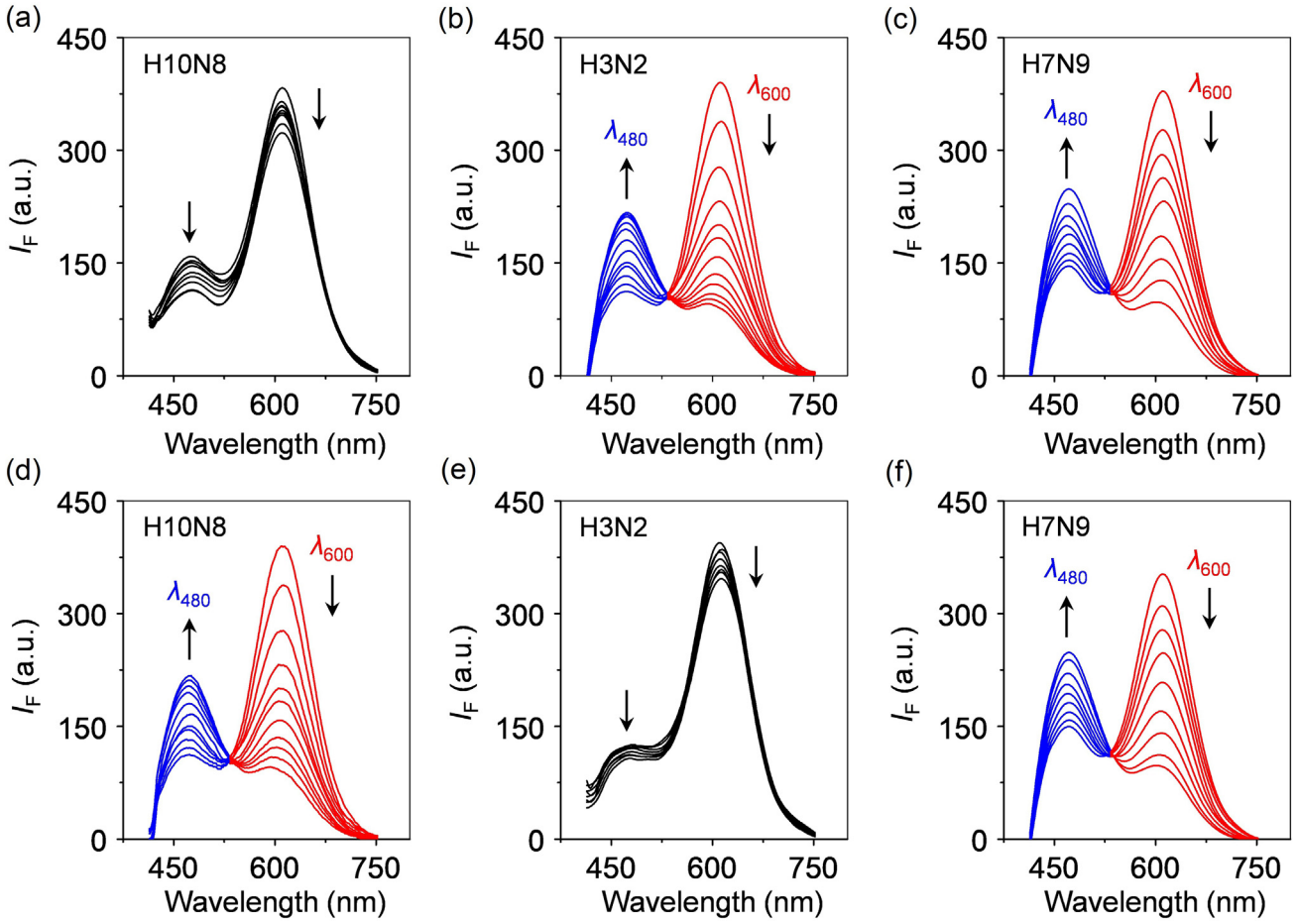

Fig. 4. (Color online) Fluorescence ratiometric change of **VR**/**DCM26** probe (10 μmol/L/10 μmol/L) in the presence of increasing (a) H10N8, (b) H3N2 and (c) H7N9 influenza virus strains in PBS (0.01 mol/L, pH 7.4). Fluorescence ratiometric change of **VR**/**DCM23** probe (10 μmol/L/10 μmol/L) in the presence of increasing (d) H10N8, (e) H3N2 and (f) H7N9 influenza virus strains in PBS (0.01 mol/L, pH 7.4). The concentration of the IVs used ranges 0–20.48 HAU 50 μL^{-1}; excitation wavelength = 365 nm.

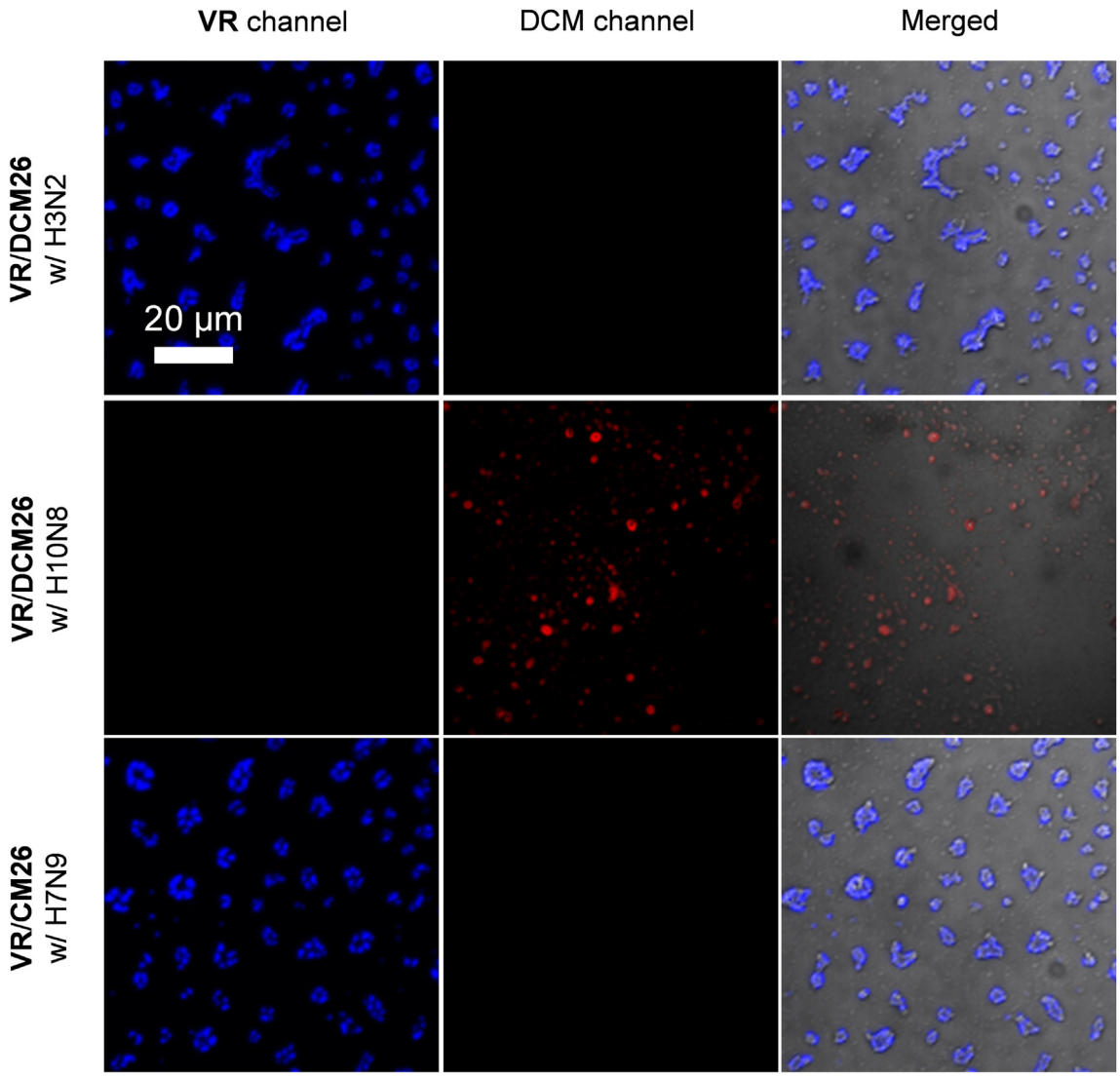

Fig. 5. (Color online) CLSM images of **VR**/**DCM26** probe (10 μmol/L/10 μmol/L) in the presence of influenza virus including H3N2, H7N9 and H10N8 with different HA specificity. The concentration of the IVs used is 20.48 HAU 50 μL^{-1}. The excitation channel used is 405 nm; the emission channel used for **VR** and DCM is 500–550 nm and 570–620 nm, respectively.

probes for IVs is dependent on their sialyllactosyl shell specificity (i.e., H3N2 and H10N8 for **DCM26** and **DCM23**, respectively, and H7N9 for both). We also determined that the ratiometric response of the probes for IVs showed good linearity over a wide concentration range (Fig. S6 online), and that the presence of a range of other viruses including AdC68 (simian adenovirus) and AdChu7 (human adenovirus), and proteins including bovine serum albumin, pepsin, lysozyme and immunoglobin G caused minimal fluorescence ratiometric change of the probes (Fig. S7 online). To further corroborate the selectivity of the probes developed, two other IV strains including H5N1 (avian influenza, A/environment/Hunan/6-69/2008) and H1N1pdm09 (human influenza, A/California/08/2009) were used. We determined that the **VR**/**DCM26** and **VR**/**DCM23** probe only showed a ratiometric fluorescence change with H1N1pdm09 and H5N1, respectively (Fig. S8 online). This again suggests the good selectivity of the core-shell probes constructed.

The effective sensing performances of the probes based on sialylglycan-HA recognition prompted us to explore their potential for blocking the IVs from invading host cells. A human lung cancer cell line (A549) that is known to highly express α2,6-sialylglycans as a receptor for human IVs [36] was used as the cell model. Human IV H3N2 stained by a known membrane-staining dye (DiL) was used for infection. After treatment of the cells with DiL-stained H3N2 viruses, a strong fluorescence was observed (Fig. 6a and b). Then, we observed that pre-treatment of the dye-labelled viruses with **DCM26** (for blocking of HA) but not **DCM23** led to a slight decrease of DiL fluorescence in cells. Remarkably, the use of the **VR**/**DCM26** probe significantly suppressed the virus fluorescence in A549 cells. This might be the result of multivalent display of the α2,6-sialyllactosides on the surface of the probes, enhancing their capacity to neutralize IVs [37]. Meanwhile, the observation that **VR** aggregates alone had a blocking effect on the IV infection agrees with the microscopic observation that blue-emitting **VR** dots were adhered to the surface of IVs (Fig. 5). Therefore, we ascribe the strong blocking effect of the **VR**/**DCM26** probe to the strong neutralization effect of the multivalently displayed **DCM26** sialyllactosides and the binding of **VR** aggregates with the surface of H3N2 IVs. The exact mechanism of action for the interaction between **VR** and IVs, which is not the major focus of the present study, remains to be delineated in the future,

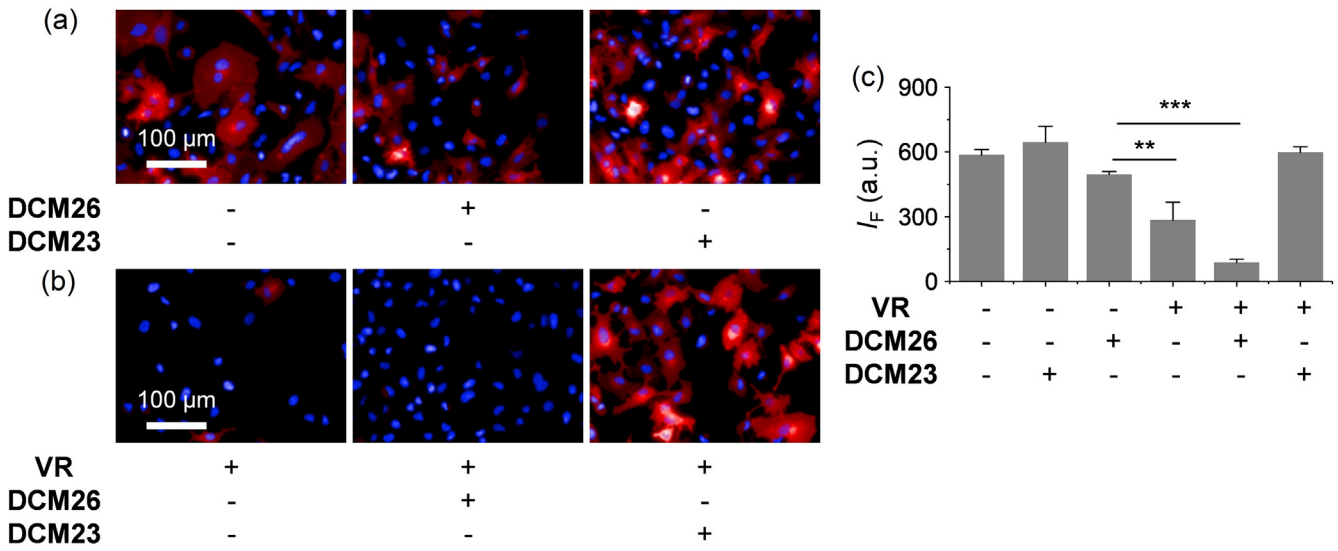

Fig. 6. (Color online) Fluorescence imaging of a human lung cancer cell ling (A549) treated with DiL-labelled H3N2 (8 HAU 50 μL^{-1}) influenza virus strain with or without preincubation of the IVs with (a) **DCM26** (10 μmol/L) and **DCM23** (10 μmol/L), and (b) **VR** alone (1 μmol/L), **VR**/**DCM26** probe (10 μmol/L/10 μmol/L) and **VR**/**DCM23** probe (10 μmol/L/10 μmol/L). (c) Fluorescence quantification of the imaging results from panels (a) and (b). The excitation and emission channel used for DiL are 520–550 nm and 560–630 nm, respectively. Cell nuclei are stained by Hoechst 33342 (excitation channel and emission channel used are 360–440 nm and 560–630 nm, respectively). Error bars mean S.D. $^{**}P < 0.01$, $^{***}P < 0.001$.

however. With a preliminary cell proliferation assay, we determined that the probes developed were not toxic to A549 cells (Fig. S9 online), highlight their potential for further biological studies.

4. Conclusions

Through pure small-molecule self-assembly, we have made possible the simple development of a new class of core-shell particle-like supramolecular probes for the ratiometric detection and blocking of IVs. Our main findings of this study include the following points. (1) **VR** aggregates, characteristic of vibration-induced emission (VIE) shift, are suitable as a molecular core structure, on which other hydrophobic (or amphiphilic) molecules can be spontaneously coated, for the construction of self-assembled fluorescence probes. (2) The core-shell self-assembly enabled the simple production of purely small-molecule fluorescence ratiometric probes if dyes with proper photophysical properties (e.g., absorption and emission) are used for functionalization of **VR** aggregates. (3) Because of the non-covalent nature of the probes, the interaction of the biomolecular ligand (in the present study glycans) shell with a target protein leads to the selective disassembly of the probe, thus making possible the ratiometric sensing; notably, the self-assembled probe remained stable in the presence of unselective species. (4) Owing to the multivalent display of biomolecular ligands to enhance the binding with protein targets, the probes are also suitable for antagonizing the selective recognition between surface-bound proteins on pathogens and receptors on host cells. We believe that his study will provide insight into the development of other functional probes with aggregation-enhanced properties by making use of exquisitely designed fluorogens.

Conflict of interest

The authors declare that they have no conflict of interest.

Acknowledgments

This work was supported by the National Natural Science Foundation of China (21788102, 91853201, 21722801, and 21776078), the Shanghai Municipal Science and Technology Major Project (2018SHZDZX03), and the National Postdoctoral Program for Innovative Talents (BX20190115).

Author contributions

Xiao-Peng He and Dong-Ming Zhou conceived idea and supervised research. Wei-Tao Dou, Zhao-Yang Qin and Jun Li conducted experiments, analyzed data and wrote the manuscript. Xiao-Peng He and Dong-Ming Zhou edited the manuscript.

Appendix A. Supplementary data

Supplementary data to this article can be found online at https://doi.org/10.1016/j.scib.2019.08.020.

References

[1] Krammer F, Smith GJD, Fouchier RAM, et al. Influenza. Nat Rev Dis Primers 2018;4:1–21.
[2] Long JS, Mistry B, Haslam SM, et al. Host and viral determinants of influenza A virus species specificity. Nat Rev Microbiol 2019;17:67–81.
[3] Xiong X, Martin SR, Haire LF, et al. Receptor binding by an H7N9 influenza virus from humans. Nature 2013;499:496–9.
[4] Zhu H, Wang D, Kelvin DJ, et al. Infectivity, transmission, and pathology of human-isolated H7N9 influenza virus in ferrets and pigs. Science 2013;341:183–6.
[5] Parrish CR, Kawaoka Y. The origins of new pandemic viruses: the acquisition of new host ranges by canine parvovirus and influenza A viruses. Annu Rev Microbiol 2005;59:553–86.
[6] Amonsen M, Smith DF, Cummings RD, et al. Human parainfluenza viruses hPIV1 and hPIV3 bind oligosaccharides with α2-3-linked sialic acids that are distinct from those bound by H5 avian influenza virus hemagglutinin. J Virol 2007;81:8341–5.
[7] García-Sastre A, Schmolke M. Avian influenza A H10N8-A virus on the verge. Lancet 2014;383:676–7.
[8] Suzuki Y, Ito T, Suzuki T, et al. Sialic acid species as a determinant of the host range of influenza A viruses. J Virol 2000;74:11825–31.
[9] Ginocchio CC, Zhang F, Manji R, et al. Evaluation of multiple test methods for the detection of the novel 2009 influenza A (H1N1) during the New York City outbreak. J Clin Virol 2009;45:191–5.
[10] Xu H, Cao W, Zhang X. Selenium-containing polymers: promising biomaterials for controlled release and enzyme mimics. Acc Chem Res 2013;46:1647–58.
[11] You L, Zha D, Anslyn EV. Recent advances in supramolecular analytical chemistry using optical sensing. Chem Rev 2015;115:7840–92.

[12] Peng H-Q, Niu L-Y, Chen Y-Z, et al. Biological applications of supramolecular assemblies designed for excitation energy transfer. Chem Rev 2015;115:7502–42.
[13] Webber MJ, Appel EA, Meijer EW, et al. Supramolecular biomaterials. Nat Mater 2016;15:13–26.
[14] Yang Y, Liu H, Han M, et al. Multilayer Microcapsules for FRET analysis and two-photon-activated photodynamic therapy. Angew Chem Int Ed 2016;55:13538–43.
[15] Wei C, Du Y, Liu Y, et al. Organic Janus microspheres: a general approach to all-color dual-wavelength microlasers. J Am Chem Soc 2019;141:5116–20.
[16] Zhang X, Chen Y, Ding SN. Facile and large-scale synthesis of green-emitting carbon nanodots from aspartame and the applications for ferric ions sensing and cell imaging. Sci Bull 2017;62:1256–66.
[17] Yu W, Guo B, Zhang H, et al. NIR-II fluorescence *in vivo* confocal microscopy with aggregation-induced emission dots. Sci Bull 2019;64:410–6.
[18] Wagner W, Wehner M, Stepanenko V, et al. Living supramolecular polymerization of a perylene bisimide dye into fluorescent J-aggregates. Angew Chem Int Ed 2017;56:16008–12.
[19] Sarkar A, Dhiman S, Chalishazar A, et al. Visualization of stereoselective supramolecular polymers by chirality-controlled energy transfer. Angew Chem Int Ed 2017;56:13767–71.
[20] Zhang M, Yin S, Zhang J, et al. Metallacycle-cored supramolecular assemblies with tunable fluorescence including white-light emission. Proc Natl Acd Sci USA 2017;114:3044–9.
[21] Zhao M, Li B, Wang P, et al. Supramolecularly engineered NIR-II and upconversion nanoparticles in vivo assembly and disassembly to improve bioimaging. Adv Mater 2018;30:1804982.
[22] Chen X-M, Chen Y, Yu Q, et al. Supramolecular assemblies with near-infrared emission mediated in two stages by cucurbituril and amphiphilic calixarene for lysosome-targeted cell imaging. Angew Chem Int Ed 2018;57:12519–23.
[23] Guo S, Song Y, He Y, et al. Highly efficient artificial light-harvesting systems constructed in aqueous solution based on supramolecular self-assembly. Angew Chem Int Ed 2018;57:3163–7.
[24] Song J-X, Tang X-Y, Zhou D-M, et al. A fluorogenic 2D glycosheet for the simultaneous identification of human- and avian-receptor specificity in influenza viruses. Mater Horiz 2017;4:431–6.
[25] .Wang C-Z, Han H-H, Tang X-Y et al. Sialylglycan-assembled supra-dots for ratiometric probing and blocking of human-infecting influenza viruses. ACS Appl Mater Interfaces 2017;9:25164–70.
[26] Zhang Z, Wu Y-S, Tang K-C, et al. Excited-state conformational/electronic responses of saddle-shaped *N,N′*-disubstituted-dihydrodibenzo[*a,c*] phenazines: wide-tuning emission from red to deep blue and white light combination. J Am Chem Soc 2015;137:8509–20.
[27] Chen W, Chen C-L, Zhang Z, et al. Snapshotting the excited-state planarization of chemically locked *N,N′*-disubstituted dihydrodibenzo[*a,c*]phenazines. J Am Chem Soc 2017;139:1636–44.
[28] Dou W-T, Chen W, He X-P, et al. Vibration-induced-emission (VIE) for imaging amyloid β fibrils. Faraday Discuss 2017;196:395–402.
[29] He X-P, Zeng Y-L, Tang X-Y, et al. Rapid identification of the receptor-binding specificity of influenza A viruses by fluorogenic glycofoldamers. Angew Chem Int Ed 2016;55:13995–9.
[30] Kenworthy AK. Imaging protein-protein interactions using fluorescence resonance energy transfer microscopy. Methods 2001;24:289–96.
[31] Eisermann J, Kerth A, Hinderberger A. Dynamic self-assembly of ions with variable size and charge in solution. RSC Adv 2019;9:18627–40.
[32] Kasson PM, Ensign DL, Pande VS. Combining molecular dynamics with bayesian analysis to predict and evaluate ligand-binding mutations in influenza hemagglutinin. J Am Chem Soc 2009;131:11338–40.
[33] Whited J, Zhang X, Nie H, et al. Recent chemical biology approaches for profiling cell surface sialylation status. ACS Chem Biol 2018;13:2364–74.
[34] Wei J, Zheng L, Lv X, et al. Analysis of influenza virus receptor specificity using glycan-functionalized gold nanoparticles. ACS Nano 2014;8:4600–7.
[35] Imai M, Kawaoka Y, et al. The role of receptor binding specificity in interspecies transmission of influenza viruses. Curr Opin Virol 2014;2:160–7.
[36] Hidari KIPJ, Yamaguchi M, Ueno F, et al. Influenza virus utilizes N-linked sialoglycans as receptors in A549 cells. Biochem Biophys Res Commun 2013;436:394–9.
[37] Ji D-K, Zhang Y, Zang Y, et al. Targeted intracellular production of reactive oxygen species by a 2D molybdenum disulfide glycosheet. Adv Mater 2016;28:9356–63.

Wei-Tao Dou received his B.Sc degree in Fine Chemistry (2013) and Ph.D. degree in Applied Chemistry (2019) with Prof. Guo-Rong Chen and Prof. Xiao-Peng He from East China University of Science & Technology (ECUST) (Shanghai, China). He's now carrying out his postdoctoral research with Prof. He Tian at ECUST, where his research interests include the development of new fluorescent probes and supramolecular ensembles for disease diagnostics and theranostics.

Xiao-Peng He (Franck) received his B.Sc degree in Applied Chemistry (2006) and Ph.D. degree in Pharmaceutical Engineering (2011). Sponsored by the French Embassy, He completed a co-tutored doctoral program at ENS Cachan (France) from July 2008 to February 2009. Then he carried out his postdoctoral research with Prof. Kaixian Chen (SIMM, CAS) at ECUST from 2011 to 2013. He's now a professor at School of Chemistry and Molecular Engineering, ECUST, where his research interests span chemical glycobiology to fluorescent molecular probes for disease diagnostics and theranostics.